Nano Today 43 (2022) 101437

Contents lists available at ScienceDirect

Nano Today

journal homepage: www.elsevier.com/locate/nanotoday

Bimetallic strip based triboelectric nanogenerator for self-powered high temperature alarm system

Jianxin Lai[a,1], Yan Ke[b,1], Zhikang Cao[a], Wenxia Xu[a], Jing Pan[a], Yifan Dong[a], Qitao Zhou[a,*], Guowen Meng[b,*], Caofeng Pan[c,**], Fan Xia[a,*]

[a] State Key Laboratory of Biogeology and Environmental Geology, Engineering Research Center of Nano-Geomaterials of the Ministry of Education, Faculty of Materials Science and Chemistry, China University of Geosciences, Wuhan 430074, China
[b] Key Laboratory of Materials Physics, and Anhui Key Laboratory of Nanomaterials and Nanotechnology, Institute of Solid State Physics, HFIPS, Chinese Academy of Sciences, Hefei 230031, China
[c] CAS Center for Excellence in Nanoscience, Beijing Key Laboratory of Micro-nano Energy and Sensor, Beijing Institute of Nanoenergy and Nanosystems, Chinese Academy of Sciences, Beijing 101400, China

ARTICLE INFO

Article history:
Received 31 December 2021
Received in revised form 11 February 2022
Accepted 17 February 2022
Available online 25 February 2022

Keywords:
Triboelectric nanogenerator
Self-powered sensor
Bimetallic strip
High temperature alarm

ABSTRACT

The failure of mechanical or electronic equipment caused by high temperature brings huge economic losses. At the same time, the potential fire danger brought by high temperature threatens people's lives. Realizing high temperature alarm is a double test of the material preparation and device construction. Here, a novel self-powered high temperature alarm sensor has been realized based on the combination of triboelectric nanogenerator and bimetallic strip. Besides, electrospun polyimide (PI) nanofiber membranes were prepared as the high temperature resistant friction material. When encountering high temperature, the rapid deformation of bimetallic strip can make it interact with the PI friction material to generate electrical signals for alarm. Finally, a series of demonstrations showed the wide application potential of the system in high temperature alarm.

Introduction

High temperature is an important cause of failure of a series of mechanical and electronic products, and also a potential source of fire hazard [1]. For example, military grade microelectronics need to work normally in the temperature range of − 55–125 ℃ [2]. Usually, people continuously monitor the temperature through the temperature sensors. When the temperature reaches the warning range, the system will alarm. In this process, these sensors need uninterrupted power supply. Therefore, it is not the best choice in the scenario where only high temperature warning is needed instead of the continuous temperature monitoring. In addition, the high temperature environment is not friendly to the integration of sensors and energy storage devices.

In recent years, the rise of triboelectric nanogenerators (TENGs) promotes the development of self-powered system. The self-powered technology based on TENGs shows great potential in distributed power sources with advantages of cost effective, light weight and high conversion efficiency. Consequently, TENGs-based self-powered systems have covered many fields, such as human motion monitoring [3–5], athletic big data analytics [6], biochemical detection [7,8], train monitoring [9] and so on. In the fields related to high temperature applications, these self-powered systems based on TENGs were mainly used in fire alarm or fire escape and rescue [10–12]. Their corresponding working principles are as follow. Most of the existing fire alarm systems based on TENGs mainly rely on TENGs to harvest the mechanical energy in the environment, such as wind energy, to power the temperature sensor or fire alarm [13–16]. For TENG-based fire escape or rescue devices, they mainly depend on the signals generated by the interaction between people and devices, rather than that generated by the device itself when exposed to high temperatures [17]. The main challenge to generate triboelectric signals under high temperature by the device itself is to find a material or design a component that can deform rapidly at a specific temperature.

* Corresponding authors.
** Correspondence to:Beijing Institute of Nanoenergy and Nanosystems, Chinese Academy of Sciences, Beijing 100083, China.
E-mail addresses: zhouqitao@cug.edu.cn (Q. Zhou), gwmeng@issp.ac.cn (G. Meng), cfpan@binn.cas.cn (C. Pan), xiafan@cug.edu.cn (F. Xia).
[1] These authors contributed equally to this work.

https://doi.org/10.1016/j.nantod.2022.101437
1748-0132/

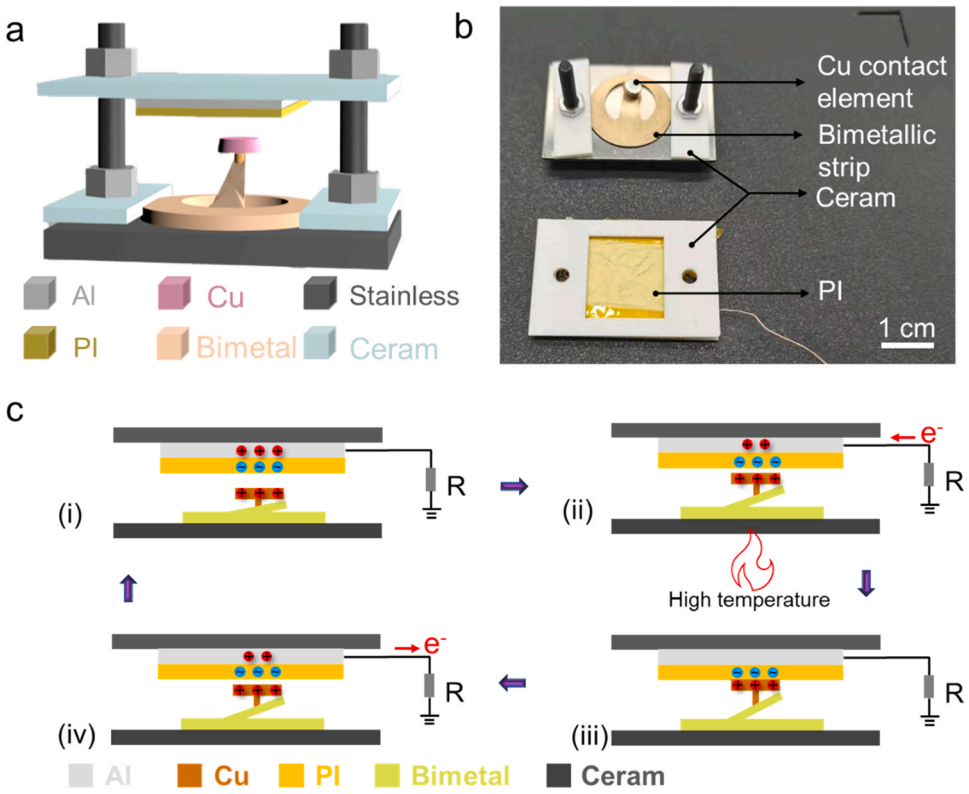

Fig. 1. Structural design and working principle of the high temperature alarm sensor. (a) Schematic illustration of the high temperature alarm sensor. (b) Photographs of the two components of the sensor: the electrification contacts material layer and the layer of the bimetallic trip. (c) Working principle of the TENG-based high temperature alarm sensor.

Fortunately, the bimetallic strip is such a material. Usually, a bimetallic strip is combined of two metallic strips with different thermal expansion coefficients which show the property to bend when the temperature changes in a specific range. Through designing the materials of the bimetallic strip, a linear deformation with temperature or a rapid deformation can be achieved based on the snap-through phenomenon. Specifically, the snap-through phenomenon refers to a rapid transition accompanied by a large shape change occurred between two equilibria of the buckled structure [18]. Accordingly, a series of applications such as temperature sensing [19], optics [20], smart actuator [21], solar tracking [22], or electromechanical breakers can be realized. Importantly, the rapid deformation of bimetallic strips caused by thermal snap-through shown a great application prospect in converting heat energy into mechanical energy [23]. Therefore, it is possible to realize high temperature alarm by combining the thermo-mechanical conversion of a bimetallic strip with a TENG.

In this study, a self-powered TENG-based high temperature alarm system is demonstrated. In this system, the high temperature alarm was realized by a TENG composed of the bimetallic strip and high temperature resistant polyimide (PI) friction material. Through the thermal snap-through of bimetallic strip at a specific temperature, the rapid deformation of bimetallic strip makes it interact with the PI friction material to generate electrical signals for alarm. Finally, a series of application demonstrations were performed to show the application potential of this system in the field of high temperature alarm.

Results and discussion

The assembling and working mechanism of TENG-based high temperature alarm system

Fig. 1a shows the schematic structure of the self-powered system based on TENG for high temperature alarm. The photo of the device is shown in Fig. 1b. Generally speaking, the device is composed of the steel sheet, bimetallic strip assembled with Cu contact element (4 mm in diameter), electrospun polyimide (PI) nanofiber membrane on Al foil and ceramic sheet assembled from bottom to top. The Cu contact element was selected as another electrode because it has a relatively positive polarity. Then the upper and lower parts were assembled together by vertical bolts and nuts.

Furtherly, the working mechanism of the device was studied. As the temperature increases, the bimetallic strip reaches its snapping temperature. At this point the center part of the dishing bimetallic strip snaps up toward the PI membrane. Thus, the Cu contact element on the center part of the dishing bimetallic strip will be in contact with the PI nanofiber membrane. Since the copper is more triboelectrically positive than PI, electrons are transferred from copper electrode on the surface of PI nanofiber membrane. Thus, the positive and negative charges are formed on the Cu contact element and the PI nanofiber membrane surface, respectively (Fig. 1c-i). Because the metal sheet has a certain elasticity, when it collides with the upper part of the device, it will bounce back and vibrate back and forth several times. The spring back of the strip will cause the separation of the Cu contact element and the PI surface, a potential difference is generated between the Al foil and ground, which can induce the transfer of charge from the Al electrode to ground (Fig. 1c-ii and c-iii). Finally, the copper contact and PI nanofiber membrane remain in contact until the bimetallic strip snaps back due to the decrease of temperature. The reason why PI nanofiber membrane is selected as friction material will be described below.

The fabrication and characterization of electrospun PI membranes

For assembling a self-powered TENG-based high temperature alarm system, the friction material should have not only good triboelectric property but also excellent thermal stability. Fortunately, PI is such a good negative friction material. Electrospinning is one of the recognized methods which could fabricate large-area ultrafine polymer nanofiber

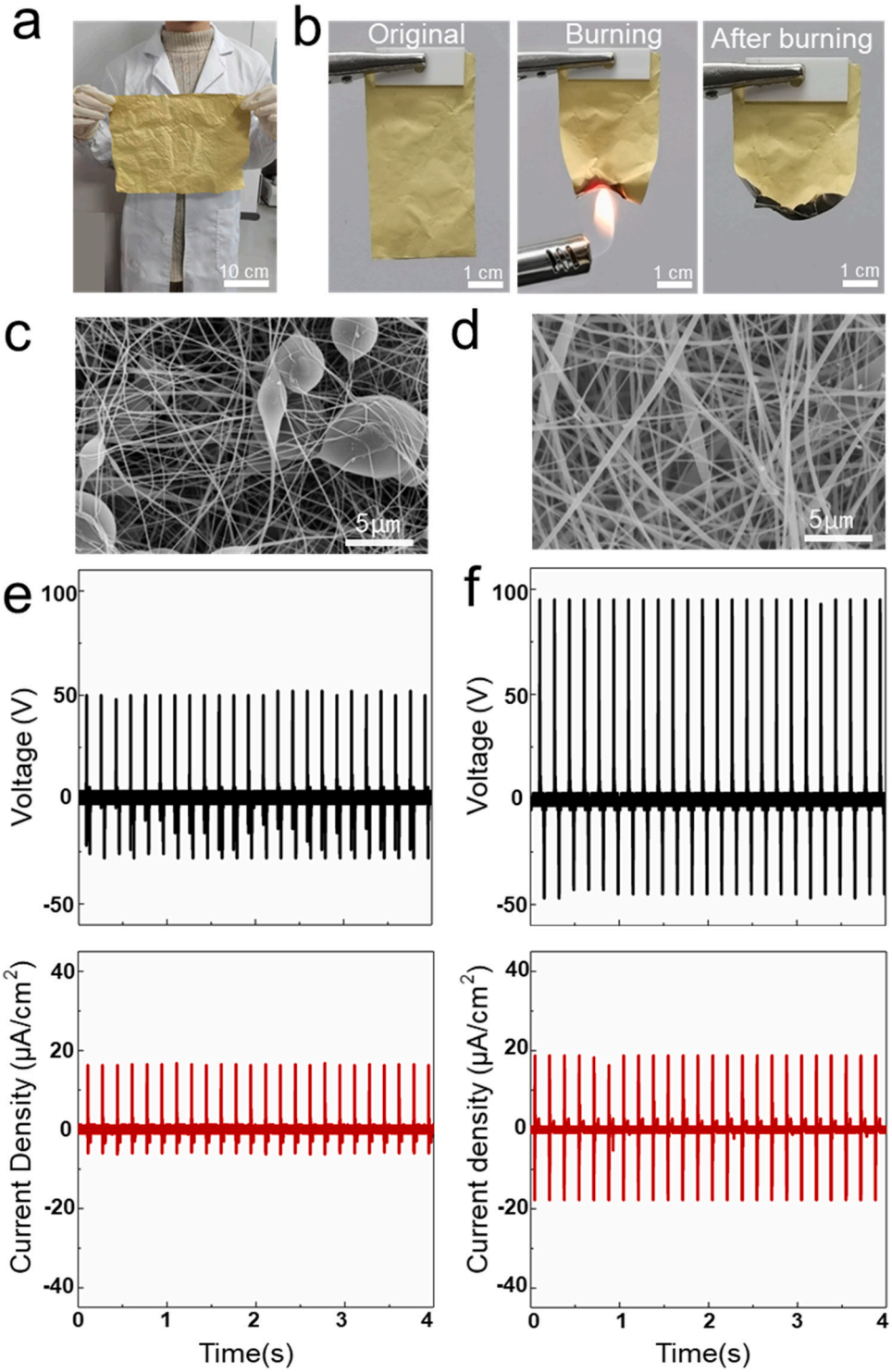

Fig. 2. Characterization of high temperature resistance ability, morphology and output properties of the prepared PI membrane. (a) Photo of the prepared PI nanofiber membranes. (b) Original, burning, and after burning photographs of the PI nanofiber membranes. (c) and (d) SEM images of PI nanofiber membranes obtained under different preparation conditions. (e) and (f) Open-circuit voltages and output current densities of TENGs with the PI nanofiber membrane corresponding to the above figures.

membranes with ultrahigh specific surface area [24]. Therefore, electrospun PI nanofiber membranes were chosen as the negative friction material here [25,26]. As shown in Fig. 2a, a PI nanofiber membrane with A4 paper size collected on the Al foil was fabricated by electrospinning of poly (amic acid) (PAA) solution and following thermal treatment. Fig. S1 shows the Fourier transform infrared (FTIR) spectrum of the as-prepared membrane. The characteristic peaks appeared at 1775 cm^{-1}, 1715 cm^{-1}, 1373 cm^{-1}, 722 cm^{-1} in nanofiber membrane, which assigned to C═O symmetric stretching vibration, C═O asymmetric stretching vibration, C–N–C stretching vibration and C–N stretch, respectively, indicated that PI was prepared [27].

Then its high temperature resistance property and morphology were also characterized. Specifically, a vertical burning test intuitively shows the flame-retardant properties of the PI/Al sample under an open fire (Fig. 2b) and demonstrates its excellent self-extinguishing ability (Movie S1). Furthermore, the morphology of PI nanofiber membranes prepared

from PAA solutions with different concentrations were compared. As seen from Fig. 2c and d, electrospun PI products transformed from bead-on-string nanofibers to bead free nanofibers with the increase of PAA concentration from 15.5 wt% to 17 wt%. When the PAA concentration is 17%, its viscoelasticity could completely suppress the Rayleigh instability induced by surface tension, resulting in bead free nanofibers. While the viscoelasticity of 15.5% PAA solution could only partially suppress the Rayleigh instability, leading to the formation of beaded nanofibers [28]. Meanwhile, the nanofiber membrane became much sparser owing to the high proportion of beads as well as low polymer concentration.

Then, a series of vertical contact–separation mode TENGs have been assembled with different PI nanofiber membranes on the Al foil interlayers as the negative-polarity triboelectric materials. And the corresponding output electrical performances were measured and compared. The vertical contact–separation mode was determined because it can easily control the triggering force or frequency, thereby minimizing experimental errors. As shown in Fig. 2e and f, both the open-circuit voltage and the current density increased when the necklace-like beaded nanofiber membrane was replaced with bead free nanofiber membrane. For the beaded nanofiber membrane-based TENG, the open-circuit voltage and the current density are 51 V and 16.2 μA/cm^2, respectively, under a mechanical percussion force of 30 N. Accordingly, the performances of the TENG assembled with a PI interlayer consisting of bead free nanofiber membrane are approximately 95 V and 18.8 μA/cm^2 under the same test condition. What's more, their performances are obviously better than that of devices prepared by commercial PI films (30 μm thick). As shown in Fig. S3, the open-circuit voltage and the current density of the TENG prepared by commercial PI tape are 15 V and 8.6 μA/cm^2, respectively. The enhancement of the electrical performance could be attributed to the larger specific surface area of the bead free PI nanofiber membrane compared with the necklace-like beaded PI nanofiber membrane [29]. In addition, to determine its effectiveness in power generation, we tested the TENG in the presence of external electrical resistance loads (Fig. S2). With the increase of electrical resistance loads from 10^4 to 10^8 Ω, the instantaneous voltage peak increased while the current density peak decreased under a force of 15 N and triggering frequency of 10 Hz, showing a trade-off phenomenon owing to the ohmic loss. As a result, the instantaneous power output per unit area reach a maximum value of 2.1 W/m^2 at an external load resistance of 10^6 Ω ($W = I^2_{peak}R$). Under the same test condition, the charge density of the vertical contact–separation mode TENG with 2 × 2 cm^2 active area is 26.6 μC/m^2 (Fig. S4a). Therefore, the bead free PI nanofiber membrane was used to prepare high temperature alarm devices owing to its excellent performances.

The performances of TENG-based high temperature alarm system

After the PI film mentioned above is assembled to obtain a self-powered sensor, the influence of the distance between the upper and lower parts of the device on the output performances of the sensor were studied. As shown in Fig. 3a, the output performance first increases and then decreases as the distance increases. To explain this result, the upper part of the device was replaced by a mechanical sensor to measure the contact force exerted on the top part by the snapping sheet. As the distance changes, the force shows a similar change as the output performance (Fig. 3b). When the

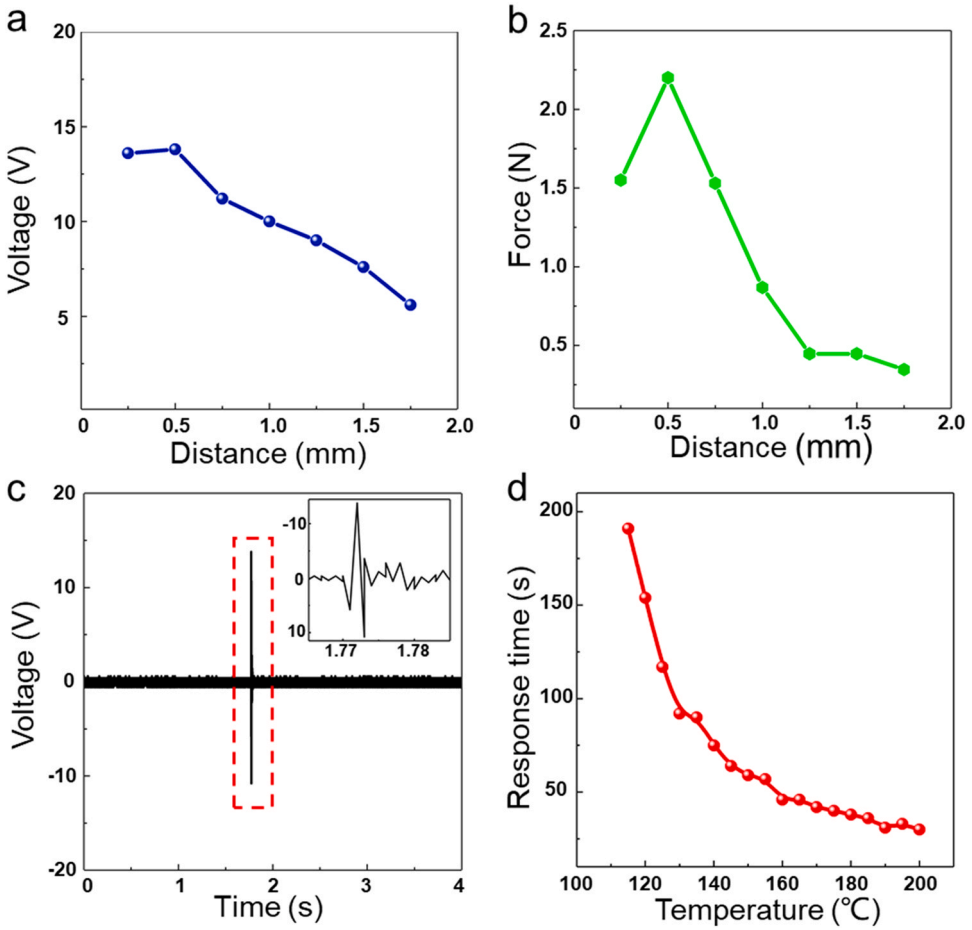

Fig. 3. Characterization of the high temperature alarm sensor. (a) The output voltages of the devices obtained by changing the distance between PI nanofiber membrane and the bimetallic strip in the device. (b) The contact force obtained by changing the distance between mechanical sensor and the bimetallic strip in the device. (c) The output voltage of the device and the corresponding enlarged picture at the optimal spacing. (d) The response time of the device at different temperatures.

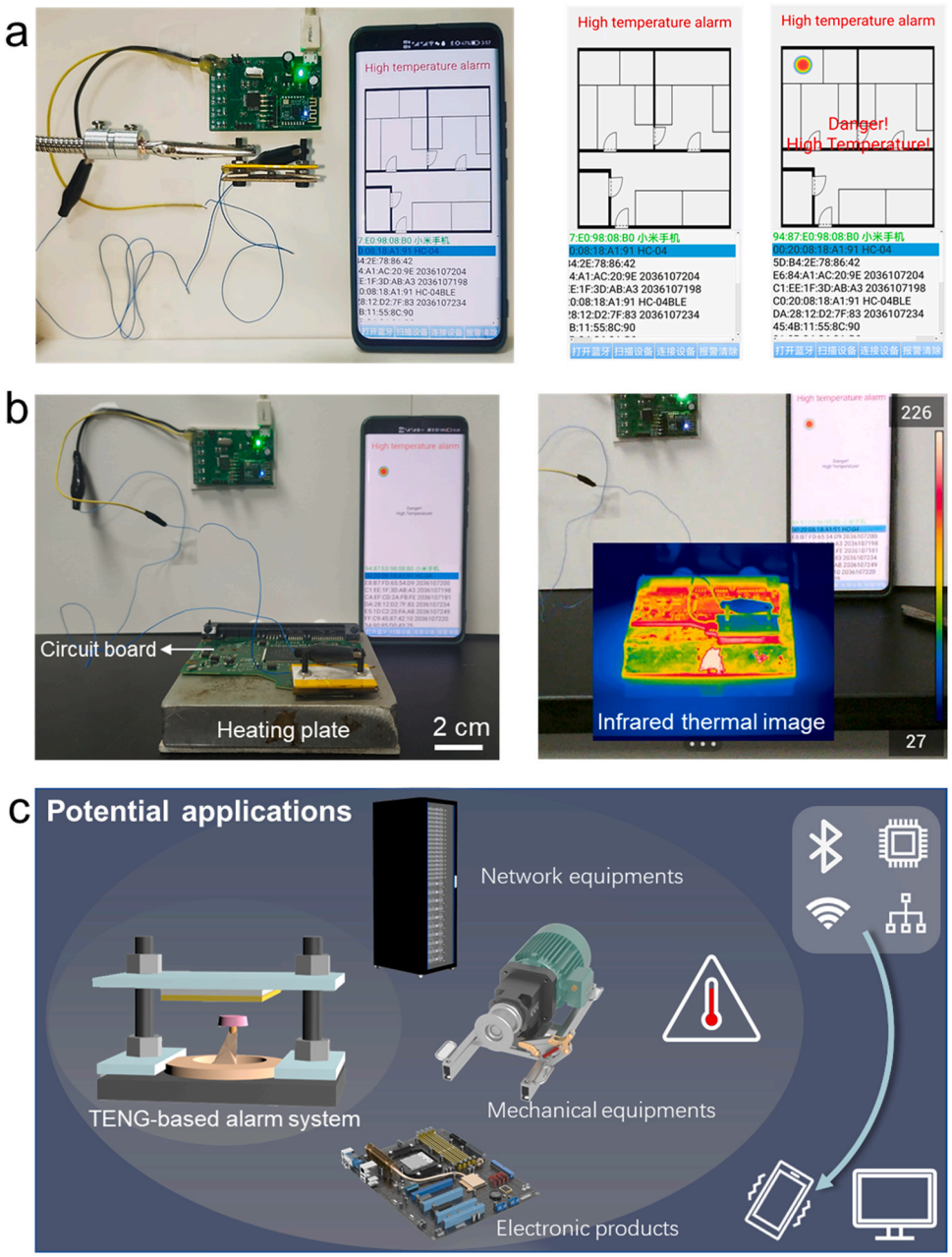

Fig. 4. The application of the high temperature alarm system. (a) The high temperature alarm system was used to locate and alarm the area with high temperature. (b) The high temperature alarm system was used to alarm the over temperature of the circuit board. (c) Schematic diagram of the application scenario of the high temperature alarm system.

distance is about 0.5 mm, the maximum open-circuit voltage can reach around 15 V (Fig. 3c). The deformation process of snapping sheet usually includes a process of acceleration and deceleration [30]. At the same time, because the contact between contact element and PI is a rapid deceleration process, the magnitude of the interaction force depends on the speed reached by contact element before contact. Therefore, when the distance is too small, the contact element will contact with PI before reaching its maximum speed, so the force generated is relatively small. When the distance continues to increase, although the maximum deformation of the snapping sheet is not exceeded, the velocity of contact element cannot has begun to decrease, and the force generated when colliding with PI also decreases accordingly. However, when the distance is greater than the maximum deformation, contact element and PI cannot collide, and the device cannot work. Therefore, the maximum pushing force is generated when the spacing is 0.5 mm, which is conducive to the interaction between the contact element and PI and increase the surface contact area, resulting in the improvement of output performance [31]. Under the optimal parameters, the charge density of the device is 14.1 $\mu C/m^2$ (Fig. S4b). In addition, the responsivity of the device was also investigated. Fig. 3d shows that the device does not respond below 120 ℃ because it has not reached the critical temperature of the thermal snap-through. However, when the temperature rises to 200 ℃, the response time of the alarm system is as low as about 20 s

The demonstration of TENG-based high temperature alarm system

Finally, a relatively complete high temperature alert system was demonstrated. The alert system includes three parts: (i) monitoring the temperature: TENG with a bimetallic strip serves as a high temperature detector to generate an electrical signal when the temperature reaches

the critical temperature; (ii) signal process and communication: a microprocessor with a Bluetooth module is used to receive and process electrical signals and send information; (iii) remote terminal, such as a cellphone or other portable electronics, to receive the emergency message of high temperature alarm. As shown in Fig. 4a, this system can realize the alarm under the direct heating of flame (Movie S2). It can be envisaged that the alarm for the high-temperature area can be realized when the alarm systems are arranged at different positions in the room. Then TENG-based self-powered high temperature alarm was combined with a circuit board. And a heating board was used to simulate the overheating of the circuit board. It could be found that when the temperature of the circuit board continued to rise to the dangerous temperature, the system could implement an alarm (Fig. 4b and Movie S3). Importantly, through the general network and intelligent terminal, family members and fire departments could be quickly informed that the temperature of the monitored equipment is too high and the fire hazard may occur. Therefore, this system is expected to be widely applied in the computer room, motor or engine, circuit board and other places that need the high temperature early warning (Fig. 4c).

Conclusions

Here, we demonstrated a TENG-based self-powered high temperature alarm sensor. The high temperature resistant PI nanofiber membrane was selected as the friction material. Specifically, through the thermal snap-through of a bimetallic strip at a specific temperature, the rapid deformation of the bimetallic strip could make it interact with the PI friction material to generate electrical signals for alarm. In addition, a self-powered high temperature early warning system was obtained by combining the TENG with the signal processing and transmission. Finally, a series of possible application scenarios were demonstrated, which showed the wide application potential of this system in the field of high temperature alarm.

Experimental section

Reagents and materials

PI nanofibers were fabricated as the high temperature resistant friction material by electrospinning of poly(amic acid) (PAA) solution and following thermal treatment [32]. The PAA/N, N-dimethylformamide (DMF) solution as the precursor solution was provided by the Changzhou Furunte Plastic New Material Co. Ltd. (China). First, the as-received PAA solution was diluted to 15.5 wt% and 17 wt% for electrospinning, respectively. Then, the electrospinning experiments were carried at the working voltage of 16 kV and tip-to-receiver distance of 15 cm with a piece of Al foil as the receiver to collect PAA nanofibers. The flow rate of PAA solutions was set as 0.8 mL/h. Finally, the as-prepared PAA nanofibers were converted to PI nanofibers through thermal treatment under four heating steps at 100 ℃, 150 ℃, 200 ℃, and 250 ℃, each for 30 min.

Preparation of TENG-based high temperature alarm system

The bottom part of the device was composed of a stainless steel sheet as the structural material with a dishing bimetallic strip fixed on it by two pieces of ceramics. For the upper part of the device, an electrospun PI nanofiber membrane on aluminum foil was used as the friction material and electrode. And the PI/Al membrane was fixed in two insulating ceramic sheets. In addition, the middle of the ceramic plate at the lower part is hollowed out to ensure that the friction material can contact with the bimetallic strip.

Characterization

The morphologies of as-prepared PI nanofiber membranes were analyzed with a field-emission scanning electron microscope (FE-SEM) (S-4800, Hitachi, Tokyo, Japan). To test the TENG property, the vertical compressive force was created by a shaker (ET-126–4, Labworks Inc., Costa Mesa, CA, USA). And the electrical measurements were performed by a low-noise current preamplifier (SR570, Stanford Research Systems, Inc., Sunnyvale, CA, USA) and a digital phosphor oscilloscope (DPO 3052, Tektronix, Inc., Beaverton, OR, USA). Besides, the infrared thermal image was recorded by using a FLIR E85 photothermal camera (FLIR Systems, Inc., Wilsonville, USA). The charge density from the output signals was measured using an electrometer (Keithley 6514, Cleveland, OH, USA).

CRediT authorship contribution statement

Q.Z., F.X. conceived the idea. Q.Z., J. L., Y. K., Z. C., S. C., J.P., Y. D., G. M., C.P. and F.X. discussed the outline and wrote the manuscript. All authors reviewed and approved the manuscript.

Declaration of Competing Interest

The authors declare that they have no known competing financial interests or personal relationships that could have appeared to influence the work reported in this paper.

Acknowledgements

This work was supported by the National Natural Science Foundation of China (22004112, 22090050, 21874121, 51902296, 52125205, U20A20166, 61805015 and 61804011), the National Key R & D Program of China (2021YFA1200403, 2018YFE0206900), the Joint NSFC-ISF Research Grant Program (Grant No: 22161142020), the Hubei Provincial Natural Science Foundation of China (2020CFA037), Zhejiang Provincial Natural Science Foundation of China under Grant No. LD21B050001.

Appendix A. Supporting information

Supplementary data associated with this article can be found in the online version at doi:10.1016/j.nantod.2022.101437.

References

[1] R. Bahru, M.F.M.A. Zamri, A.H. Shamsuddin, N. Shaari, M.A. Mohamed, A review of thermal interface material fabrication method toward enhancing heat dissipation, Int. J. Energy Res. 45 (2021) 3548–3568.
[2] M. Ohadi, J. Qi, Thermal Management Of Harsh Environment Electronics, Springer, Dordrecht, Netherlands, 2005.
[3] L. Huang, S. Lin, Z. Xu, H. Zhou, J. Duan, B. Hu, J. Zhou, Fiber-based energy conversion devices for human-body energy harvesting, Adv. Mater. 32 (2020) 1902034.
[4] F. Wen, Z. Sun, T. He, Q. Shi, M. Zhu, Z. Zhang, L. Li, T. Zhang, C. Lee, Machine learning glove using self-powered conductive superhydrophobic triboelectric textile for gesture recognition in VR/AR applications, Adv. Sci. 7 (2020) 2000261.
[5] T. He, Q. Shi, H. Wang, F. Wen, T. Chen, J. Ouyang, C. Lee, Beyond energy harvesting - multi-functional triboelectric nanosensors on a textile, Nano Energy 57 (2019) 338–352.
[6] J. Luo, Z. Wang, L. Xu, A.C. Wang, K. Han, T. Jiang, Q. Lai, Y. Bai, W. Tang, F.R. Fan, Flexible and durable wood-based triboelectric nanogenerators for self-powered sensing in athletic big data analytics, Nat. Commun. 10 (2019) 5147.
[7] Q. Zhou, K. Lee, S. Deng, S. Seo, F. Xia, T. Kim, Meso-scale modeling and damage analysis of carbon/epoxy woven fabric composite under in-plane tension and compression loadings, Nano Energy 85 (2021) 105980.
[8] Q. Zhou, J. Pan, S. Deng, F. Xia, T. Kim, Triboelectric nanogenerator-based sensor systems for chemical or biological detection, Adv. Mater. 33 (2021) 2008276.
[9] L. Jin, S.L. Zhang, S. Xu, H. Guo, W. Yang, Z.L. Wang, Free-fixed rotational triboelectric nanogenerator for self-powered real-time wheel monitoring, Adv. Mater. Technol. 6 (2021) 2000918.

[10] R. Cheng, K. Dong, L. Liu, C. Ning, P. Chen, X. Peng, D. Liu, Z.L. Wang, Flame-retardant textile-based triboelectric nanogenerators for fire protection applications, ACS Nano 14 (2020) 15853–15863.
[11] L. Ma, R. Wu, S. Liu, A. Patil, H. Gong, J. Yi, F. Sheng, Y. Zhang, J. Wang, J. Wang, A Machine-fabricated 3D honeycomb-structured flame-retardant triboelectric fabric for fire escape and rescue, Adv. Mater. 32 (2020) 2003897.
[12] P. Sun, N. Cai, X. Zhong, X. Zhao, L. Zhang, S. Jiang, Facile monitoring for human motion on fireground by using MiEs-TENG sensor, Nano Energy 89 (2021) 106492.
[13] X. Zhang, J. Hu, Q. Yang, H. Yang, H. Yang, Q. Li, X. Li, C. Hu, Y. Xi, Z.L. Wang, Harvesting multidirectional breeze energy and self-powered intelligent fire detection systems based on triboelectric nanogenerator and fluid-dynamic modeling, Adv. Funct. Mater. 31 (2021) 2106527.
[14] W. Liu, X. Wang, Y. Song, R. Cao, L. Wang, Z. Yan, G. Shan, Biomechanically reduced expression of Derlin-3 is linked to the apoptosis of chondrocytes in the mandibular condylar cartilage via the endoplasmic reticulum stress pathway, Nano Energy 73 (2020) 104843.
[15] J. Mu, J. Zou, J. Song, J. He, X. Hou, J. Yu, X. Han, C. Feng, H. He, X. Chou, Hybrid enhancement effect of structural and material properties of the triboelectric generator on its performance in integrated energy harvester, Energy Convers. Manag. 254 (2022) 115151.
[16] X. Gao, F. Xing, F. Guo, Y. Yang, Y. Hao, J. Chen, B. Chen, Z.L. Wang, A turbine disk-type triboelectric nanogenerator for wind energy harvesting and self-powered wildfire pre-warning, Mater. Today Energy 22 (2021) 100867.
[17] H. He, J. Liu, Y. Wang, Y. Zhao, Y. Qin, Z. Zhu, Z. Yu, J. Wang, The development and validation of simplified machine learning algorithms to predict prognosis of hospitalized patients With COVID-19: multicenter, retrospective study, ACS Nano 24 (2022) 31549.
[18] H. Kim, Q. Zhou, D. Kim, I.K. Oh, Flow-induced snap-through triboelectric nanogenerator, Nano Energy 68 (2020) 104379.
[19] X. Shi, F. Yang, S. Xu, M. Li, Pallidin protein in neurodevelopment and its relation to the pathogenesis of schizophrenia, Sensors 17 (2017) 665–672.
[20] K. Tian, Y. Liu, Q. Wang, Temperature-independent fiber Bragg grating strain sensor using bimetal cantilever, Opt. Fiber Technol. 11 (2005) 370–377.
[21] C. Li, W. Ouyang, H. Guo, D. Tang, R. Liu, Z. Deng, Concept and preliminary design of SMA bimetallic strip smart actuator for space adaptive structures, Mater. Res. Express 6 (2019) 115710.
[22] Z. Zhang, K. Pei, M. Sun, H. Wu, X. Yu, H. Wu, S. Jiang, F. Zhang, A novel solar tracking model integrated with bistable composite structures and bimetallic strips, Compos. Struct. 248 (2020) 112506.
[23] A. Arnaud, J. Boughaleb, S. Monfray, F. Boeuf, O. Cugat, T. Skotnicki, Thermo-mechanical efficiency of the bimetallic strip heat engine at the macro-scale and micro-scale, J. Micromech. Microeng. 25 (2015) 104003.
[24] Y. Li, J. Zhu, H. Cheng, G. Li, H. Huo, M. Jiang, Q. Gao, X. Zhang, Developments of advanced electrospinning techniques: a critical review, Adv. Mater. Technol. 6 (2021) 2100410.
[25] Y. Kim, X. Wu, J.H. Oh, Fabrication of triboelectric nanogenerators based on electrospun polyimide nanofibers membrane, Sci. Rep. 10 (2020) 2742.
[26] S. Jiang, B. Uch, S. Agarwal, A. Greiner, Ultralight, thermally insulating, compressible polyimide fiber assembled sponges, ACS Appl. Mater. Interfaces 9 (2017) 32308–32315.
[27] C. Luo, X. Wang, J. Wang, K. Pan, One-pot preparation of polyimide/Fe 3 O 4 magnetic nanofibers with solvent resistant properties, Compos. Sci. Technol. 133 (2016) 97–103.
[28] C. Luo, M. Edirisinghe, Core-liquid-induced transition from coaxial electrospray to electrospinning of low-viscosity poly(lactide-co-glycolide) sheath solution, Macromolecules 47 (2014) 7930–7938.
[29] Q. Zhou, K. Lee, K.N. Kim, J.G. Park, J. Pan, J. Bae, J.M. Baik, T. Kim, Activating adiponectin signaling with exogenous adiporon reduces myelin lipid accumulation and suppresses macrophage recruitment after spinal cord injury, Nano Energy 57 (2019) 903–910.
[30] Y. Kim, J. van den Berg, A.J. Crosby, Autonomous snapping and jumping polymer gels, Nat. Mater. 20 (2021) 1695–1701.
[31] B. Dudem, N.D. Huynh, W. Kim, D.H. Kim, H.J. Hwang, D. Choi, J.S. Yu, Nanopillar-array architectured PDMS-based triboelectric nanogenerator integrated with a windmill model for effective wind energy harvesting, Nano Energy 42 (2017) 269–281.
[32] D. Wang, J. Yu, G. Duan, K. Liu, H. Hou, Electrospun polyimide nonwovens with enhanced mechanical and thermal properties by addition of trace plasticizer, J. Mater. Sci. 55 (2020) 5667–5679.